FIXED-BED ADSORPTION OF CONGO RED ONTO TEA WASTE IN THE PRESENCE OF Fe_2O_3 NANOPARTICLES: AN EXPERIMENTAL AND MODELING STUDY

Mohammad Foroughi-dahr[1], Hossein Abolghasemi[1,2]*, Mohamad Esmaili[1], Alireza Shojamoradi[1], and Hooman Fatoorehchi[1]

[1] Center for Separation Processes Modeling and Nano-Computations, School of Chemical Engineering, College of Engineering, University of Tehran, P.O. Box 11365-4563, Tehran, Iran

[2] Oil and Gas Center of Excellence, University of Tehran, Tehran, Iran

ABSTRACT

In this study, tea waste (TW) is employed for the removal of Congo red (CR) from aqueous solutions in a fixed-bed column at 30 °C. The breakthrough curves of the adsorption process of CR on TW at three different flow rates are determined. The results revealed that the breakthrough curves were dependent on flow rates in a manner in which a lower flow rate was in favor of the CR adsorption in the column-mode process. As the flow rate increased from 4.6 to 6.6 mL/min, the amount of dye uptake capacity decreased from 1.78 to 1.53 mg/g. The effect of the presence of Fe_2O_3 on the adsorption of CR on TW is also studied at 30 °C. The results showed that the presence of nanoparticles increased the adsorption uptake of CR by about 32%. Moreover, four novel models are developed for the prediction of the breakthrough curves resulted from the experimental data. The results of the models were in good agreement with experimental data (R^2>0.99). The statistical parameters confirm the suitability of the models.

Keywords: Tea Waste, Congo Red, Adsorption, Fixed-bed Column, Breakthrough Modeling, Fe_2O_3 Nanoparticles

INTRODUCTION

Nowadays, large amounts of pollutants are being used in modern industries. The widespread use of dyes in various industries has made them of great environmental concern due to both toxicological and esthetical reasons [1,2]. Dye wastewaters are too toxic and may cause a serious hazard on aquatic organisms. Most of the dyes are originally synthetic and their structure contains complex aromatic rings which make them stable and difficult to be degraded biologically. As a matter of fact, the low biodegradability of dyes makes the conventional treatment to be inefficient. Hence physical and chemical treatments are required [3,4]. Adsorption processes have proved to be suitable for the removal of dye pollutants from wastewaters [5,6]. Activated carbon has been widely used as convenient adsorbent for the removal of dyes from wastewaters [7]. However, the expensive cost of activated carbon and its regeneration process have made some difficult-

***Corresponding author**

Hossein Abolghasemi

Email: hoab@ut.ac.ir

Tel: +98 21 6695 4051

Fax: +98 21 6111 2186

Article history

Received: April 8, 2013

Received in revised form: June 16, 2013

Accepted: June 17, 2013

Available online: October 25, 2013

© 2013 Research Institute of Petroleum Industry (RIPI)

ties for the adsorption to be an economic treatment process. In reality, the adsorption process profitably depends on the price of the adsorbent and the simplicity of its use. Several low cost adsorbents, including peanut hull [8], maize stalk [9], rice husk [10], chitosan composite [11], broad bean peels [12], etc. have been investigated to study the adsorption performance for the removal of dyes from aqueous solutions. Congo red (CR) is a benzidine-based anionic diazo dye which is known to cause allergic reactions. The azo dyes are characterized by the presence of at least one azo group consisting of nitrogen-nitrogen double bonds.

There are numerous batch adsorption studies in the literature, but there are not enough studies on the fixed-bed column process. However, industrial processes require the continuous treatment systems. In fact, the fixed-bed adsorption studies are more useful and practical for industrial goals [13]. Tea plants are commonly cultivated in the northern area of Iran. Tea waste (TW) has been used for the removal of several heavy metals and dyes from aqueous solutions. Amarasinghe and Williams applied tea waste for the adsorption of copper and plumb from aqueous solutions with an adsorption capacity of 48 and 65 mg/g respectively [14]. Wasewar et al. used tea factory waste for the removal of zinc from aqueous solutions with a maximum adsorption capacity of 8.9 mg/g [15]. Malkoc and Nuhoglu investigated the adsorption of nickel(II), in which the adsorption capacity was found to be 18.42 mg/g [16]. Hameed used spent tea leaves for the removal of methylene blue from aqueous solution with an adsorption capacity of 300.052 mg/g [17].

Nanofluids are defined as fluids with dispersed nanoparticles smaller than 100 nm in diameter, in which the nanoparticles are stably suspended in the base fluid [18]. Many researchers have investigated the effect of different nanoparticles on base fluid materials because of the great features of nanoparticles which can be attributed to their small size and large specific surface area [19]. The effects of nanoparticles on heat thermal conductivity are investigated by investigators [20,21]. Furthermore, the effects of nanoparticles on the mass transfer in the liquid phase have been investigated in several works. Krishnamurthy et al. investigated the mass diffusion of fluoresin dye in nanofluids using time-dependant images [22]. The results revealed that the dye diffusion in nanofluids was faster than in pure water. Wen et al. measured the gas-liquid mass transfer in an airlift reactor in the presence of nanoparticles [23]. It was observed that nanoparticles had a strong effect on mass transfer. In this study, the performance of TW for the removal of CR in a fixed-bed column is investigated. The effect of the presence of nanoparticles on the adsorption performance of TW for the removal of CR is studied. Finally, the modeling of the fixed-bed adsorption dynamics is presented and the model parameters are calculated.

EXPERIMENTAL

Chemicals

The CR [1-naphthalen sulfonic acid, 3, 30-(4,40-biphenylenebis (azo)) bis(4-amino)disodium salt] used in this study was supplied by Merck company. Its C.I. No. is 22120 and FW=696; its chemical formula is $C_{32}H_{22}N_6Na_2O_6S_2$, and λ_{max}=495 nm. The molecular structure of CR is illustrated in Figure 1. Fe_2O_3 nanoparticles with a BET surface area of 60 m^2/g and an average primary particle size of 40 nm were supplied by Degussa Company. The tea leaves used in this experiment were produced in tea plantations from the northern area of Iran. The tea waste (TW) was collected, and prior to the experiments, was repeatedly washed with boiled water to remove its original dye particles and other impurities until the washing water con-

© 2013 Research Institute of Petroleum Industry (RIPI)

tained no color. TW was then washed with distillated water and was oven dried for 48 hrs at 70 °C. Subsequently, the dried sample was crushed and sieved. The particle size was in the range of 125-250 μm. The prepared sample was stored in plastic bottles for further use.

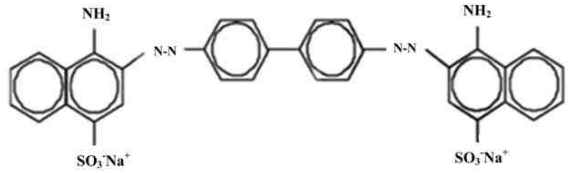

Figure 1: Molecular structure of CR

Preparation of the Adsorbent

Preparation and Stability Analysis of the Nanofluid

To prepare the nanofluids of Fe_2O_3 of 20 ppm, proper amounts of Fe_2O_3 nanoparticles was dispersed in distilled water by ultrasonication for about 1 hr (Misonix sonicator 3000). The inffluent CR solution of 30 mg/L was prepared by adding proper amount of CR to the nanofluids. The scanning electron microscopy (SEM) micrograph of the Fe_2O_3 nanoparticles is shown in Figure 2a. It can be seen from Figure 2a that Fe_2O_3 nanoparticles are spherical in physical nature. In addition, the dynamic light scattering (DLS) is illustrated in Figure 2b. The mean diameter was found to be 62 nm for Fe_2O_3 nanoparticles.

The stability of the nanofluid is an important parameter influencing the nanoparticle performance in the liquid phase; besides, the stability of the nanofluids affects the sample analyses. The stability of the present nanofluids was examined using UV-vise spectrophotometer (UNICAM, 8700 series, USA) at the nanoparticle maximum absorbance wavelength of about 649 nm. The samples were analyzed at predetermined time intervals. The relative concentrations (C/C_0) of the nanoparticles are shown in Figure 3. It can be seen that the nanofluid has perfect stability during the experiment period.

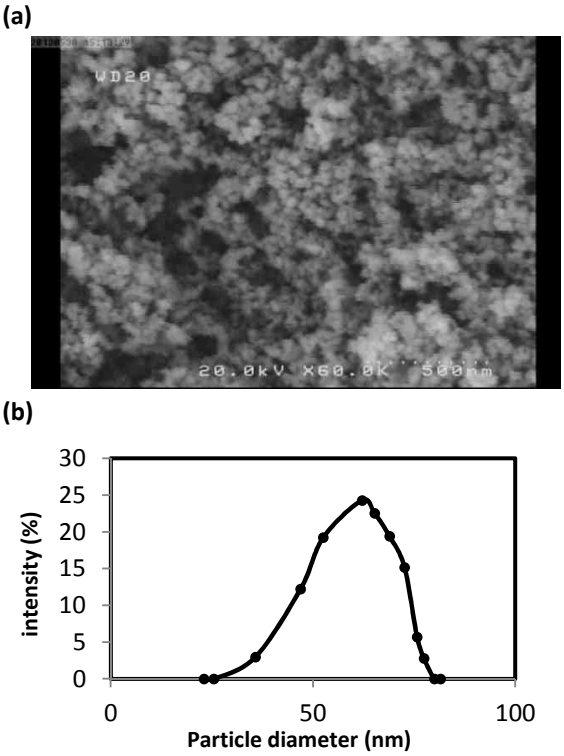

Figure 2: (a) FESEM image of Fe_2O_3 nanoparticles; (b) DLS image of Fe_2O_3 nanofluid

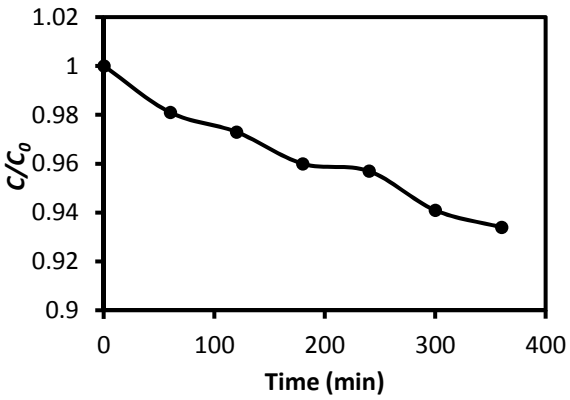

Figure 3: The nanofluid relative concentration vs. time

Experimental Set-up

A schematic diagram of the experimental setup used in this study is depicted in Figure 4. The column experiments were conducted in a glass tube with an inside diameter of 1.4 cm and a height of 20 cm. The adsorbent was supported by glass wool on the top and also the bottom of the bed to provide a uniform flow of the feed solution in the column. The column was packed with 10 g of TW (equivalent to 14.6 cm of the bed depth). The column experiments were

© 2013 Research Institute of Petroleum Industry (RIPI)

performed at different volumetric flow rates (4.6, 5.6, and 6.6 mL/min). The CR solution was fed through the bottom of the column in up-flow mode to avoid channeling of the solution using a peristaltic pump. The temperature of the feed was maintained at 30 °C by means of a water circulation heater in which water was continuously passed through a surrounding jacket around the adsorption column (Figure 5). Samples were collected periodically to determine the remaining CR concentration using a UV-vis spectrophotometer (UNICAM, 8700 series, USA) at λ_{max}=495nm.

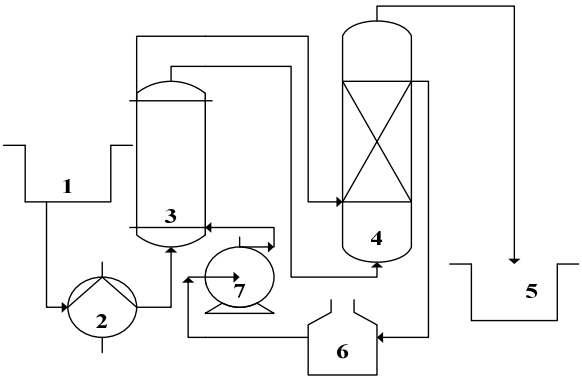

Figure 4: A schematic diagram of the packed bed column apparatus; (1) feed tank; (2) peristaltic pump; (3) shell and tube heat exchanger; (4) fixed-bed adsorption column and shell and tube exchanger; (5) product tank; (6) liquid circulator heater; (7) pump.

Fixed-bed Data Analysis

The breakthrough curve is usually expressed by the ratio of effluent concentration (C_t) to influent concentration (C_0) (C_t/C_0) as a function of time (t). The effluent volume (V_{eff}) can be calculated by Equation 1 [24]:

$$V_{eff} = Qt_{total} , \quad (1)$$

where, t_{total} and Q are the total flow time (min) and volumetric flow rate (mL/min), respectively. Total adsorbed CR quantity can be found from integrating the adsorbed concentration (C_{ad}) versus t (min) plot, i.e. the area under the breakthrough curves. The value of total adsorbed CR in the fixed-bed column for a given feed concentration and flow rate is calculated from Equation 2 [24]:

$$q_{total} = \frac{QA}{1000} = \frac{Q}{1000}\int_{t=0}^{t=t_{total}} C_{ad}\,dt , \quad (2)$$

Equilibrium uptake (q_{eq}) or maximum column capacity in the column is defined as the total amount of adsorbed dye (q_{total}) per gram of adsorbent (W) at the end of total flow time (Equation 3) [24]:

$$q_{eq} = \frac{q_{total}}{W} , \quad (3)$$

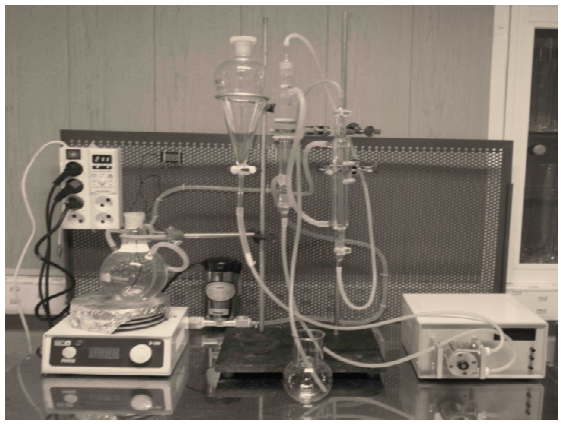

Figure 5: The laboratory fixed-bed column

RESULTS AND DISCUSSION

Fixed-bed Breakthrough Curves at Different Flow Rates

Figure 6 shows the breakthrough curves resulted from the adsorption of CR on TW at different feed rates of 4.6, 5.6, and 6.6 mL/min, with the initial dye concentration of 30 mg/L, and at a constant mass of the adsorbent of 10 g. The results are presented in Table 1. It is obvious from Figure 6 that lower flow rates give a later breakthrough curve and greater treated volume is obtained, which can be attributed to the fact that at lower flow rates the contact time between the adsorbent and the adsorbate increases in column and as a result higher removal efficiency is achieved. It can be seen from Figure 6 that the breakthrough point increases from 17.5 to 27.8 min. by reducing the

© 2013 Research Institute of Petroleum Industry (RIPI)

flow rate from 6.6 to 4.6 mL/min. According to Table 1, the dye uptake capacity decreases from 1.78 to 1.53 mg/g by increasing flow rate from 4.6 to 6.6 mL/min, which is due to the fact that the intraparticle diffusion is the dominant mechanism in the process of the adsorption of CR on TW. The results are entirely in consistence with the results of other studies given elsewhere [25-28].

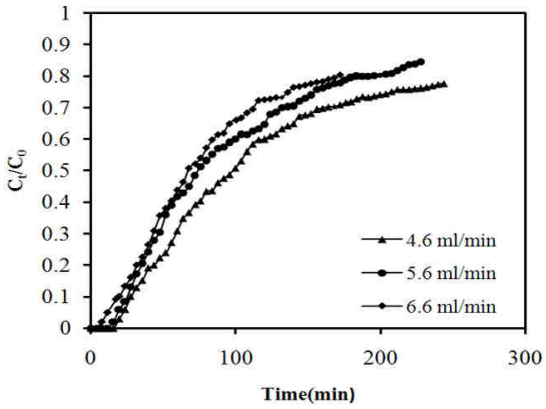

Figure 6: The effect of volumetric flow rates on the CR adsorption on TW (C_0= 30 mg/L, mass of the adsorbent= 10g, and T = 30 °C)

Table 1: The parameters of the fixed-bed column for the adsorption of CR onto TW under different conditions

Flow rate (mL/min)	q_{tot} (mg)	q_e (mg/g)
4.6	17.78	1.78
5.6	16.41	1.64
6.6	15.29	1.53

Effect of the Presence of Fe_2O_3 Nanoparticles on Dye Adsorption

The effect of nanoparticles on the fixed-bed adsorption of CR onto TW is illustrated in Figure 7. The experiments are conducted at a constant flow rate of 6.6 mL/min, the mass of the adsorbent of 10 g, and the inlet concentration of 30 mg/L in the absence of nanoparticles and in the presence of a nanoparticle concentration of 20 ppm. The temperature of the fixed-bed column was adjusted at 30 °C. The results of the influence of the presence of nanoparticles are given in Table 2. As shown in Figure 7, breakthrough curve occurs later and the saturation breakthrough time is increased in the presence of nanoparticles. According to Figure 7, by adding Fe_2O_3 nanoparticles to the influent CR solution, the related slope for the breakthrough curve significantly decreases, which results in a broadened mass transfer zone. The aforementioned results can be attributed to the effects of nanoparticles on the mass transfer of CR molecules. Several investigators have stated that the presence of nanoparticles increases the mass transfer in the liquid phase [22,23]. The velocity disturbance field in the fluid, created by the motion of the nanoparticles, may be responsible for the adsorption enhancement. From another point of view, the Brownian motion of nanoparticles makes the nanoscale stirring of the liquid increase [22]. Besides, Fe_2O_3 nanoparticles decrease the boundary layer resistance over the adsorbent particle and as a result the diffusion rate of CR through the adsorbent may be enhanced.

It can be seen from Table 2 that the adsorption capacity increases from 1.53 to 2.03 mg/g by applying the nanoparticles to the adsorption process; this means that the existence of nanoparticles increases the dye uptake capacity by about 32%.

Dynamic Modeling

Breakthrough curves manifest the concentration profiles in fixed-bed systems. As it can be seen from breakthrough curves, the concentrations of the adsorbate vary in time as well as the space of the column. Hence multivariable models have been considered for the design of such processes. Modeling the experimental data of the column studies, provide valuable information for the scale-up of the system and describing the dynamic behavior of the adsorption process [29, 30]. Several mathematical models have been developed describing the column experiments.

© 2013 Research Institute of Petroleum Industry (RIPI)

Table 2: The parameters of the fixed-bed column for the adsorption of CR onto TW under different conditions

Flow rate (ml/min)	q_{tot} (mg)	q_e (mg/g)
Adsorption in the absence of nanoparticles	20.32	2.03
Adsorption in the absence of nanoparticles	15.29	1.53

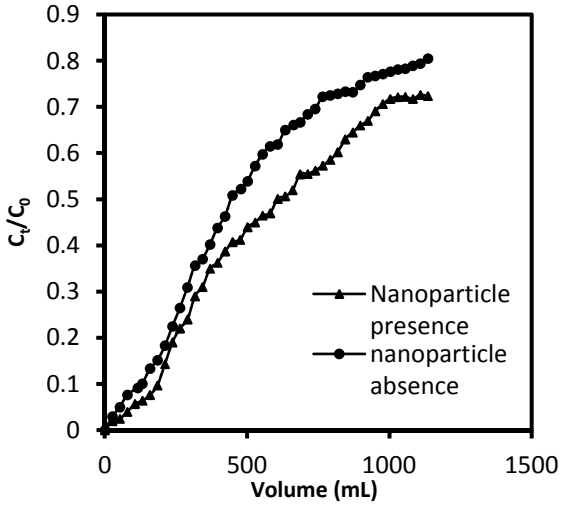

Figure 7: The effect of the presence of nanoparticles on the adsorption breakthrough curves; each point represents the mean value of three replicates.

Thomas, Asams-Bohart, Yoon-Nelson, and BDST models are the commonest ones presented in the literature [31-34]. It should be noted that the aforesaid models are suitable mostly with the assumption of local equilibrium and no axial dispersion. On the other hand, they are hardly suitable for the adsorption processes with high axial dispersion, in which their breakthrough curves are broadened.

Four different models have been proposed to predict the breakthrough curves. The mentioned models include the multiple of a multivariable function and an exponential function in order to enable the models predicting the breakthrough curves of the axially-dispersed plug flow adsorption processes. The suggested models are presented as follows:

Model (1):

$$X = \frac{C_b}{C_f} = 1 + (a_1 + a_2 t)\exp(-a_3 t) \quad (4)$$

Model (2) [35]:

$$X = \frac{C_b}{C_f} = 1 + (b_1 + b_2 t^{b_3})\exp(-b_4 t) \quad (5)$$

Model (3):

$$X = \frac{C_b}{C_f} = 1 + (d_1 + d_2 t^{d_3})\exp(-d_4 t^2) \quad (6)$$

Model (4):

$$X = \frac{C_b}{C_f} = 1 + (e_1 + e_2 t + e_3 t^2)\exp(-e_4 t^2) \quad (7)$$

where, a_1 to a_3 are the constants of model (1) (Equation 4); b_1 to b_4 stand for the constants of model (2) (Equation 5); d_1 to d_4 represent the constants of model (3) (Equation 6), and e_1 to e_4 denote the constants of model (4) (Equation 7). It is important to point out that this type of modeling of the breakthrough curves is novel and has not previously been reported in the literature. The best model well fits the experimental data acquired from the column studies. The correlation and modeling constants have been determined with respect to O.L.S. method by Eviews software. The modeling constants as well as the correlation coefficient (R^2), adjusted-R^2, and the residual sum of squares (RSS) are summarized in Table 3.

The experimental and predicted breakthrough curves of the models are shown in Figures 8-11. Equations 4-7 were applied to estimate the breakthrough curves in Figures 8-11. It can be seen from Figures 8-11 that model (4) provided the best fit for the experimental data. However, model (1) and model (2) showed good agreement with the experimental data. It can be seen from Table 3 that all the models except for model (3) have high values of R^2, adjusted-R^2, and RSS. Compared to R^2, adjusted-R^2, and RSS listed in Table 3, the values of R^2 and adjusted-R^2 from model (4) were the largest, while the values of RSS were the least (the values of R^2>0.99 and adjusted-R^2>0.99). Therefore, it can

© 2013 Research Institute of Petroleum Industry (RIPI)

be concluded that model (4) is the best model describing the adsorption behavior and can properly predict the dynamic data of the adsorption of CR onto TW in a fixed-bed column.

Table 3: The parameters of the adsorption dynamic models

Model	Flow rate (ml/min)	Model constants	R^2	Adjusted R^2	RSS
Model (1)	4.6	a_1 = -1.072, a_2 = -1.57×10^{-7}, a_3 = 0.008	0.9924	0.9921	0.213
	5.6	a_1 = -1.075, a_2 = -1.25×10^{-7}, a_3 = 0.009	0.9919	0.9915	0.247
	6.6	a_1 = -1.098, a_2 = -1.14×10^{-6}, a_3 = 0.011	0.9900	0.9895	0.0247
Model (2)	4.6	b_1 = -1.089, b_2 = 0.963, b_3 = -1.839, b_4 = 0.008	0.9938	0.9934	0.0172
	5.6	b_1 = -1.086, b_2 = 9029.03, b_3 = -8.549, b_4= 0.009	0.9929	0.9916	0.0190
	6.6	b_1 = -1.134, b_2 = 10.037, b_3 = -2.205, b_4 = 0.011	0.9922	0.9916	0.0190
Model (3)	4.6	d_1 = 33.87, d_2 = -35.18, d_3 = -0.004, d_4 = 2.47×10^{-5}	0.9709	0.9690	0.0818
	5.6	d_1 =-0.844, d_2 = 9029.3, d_3 = -27.23, d_4= 6.00×10^{-5}	0.9067	0.9004	0.2844
	6.6	d_1 = -1.489, d_2 = 0.237, d_3 = 0.318, d_4 = 2.00×10^{-5}	0.9800	0.9784	0.0491
Model (4)	4.6	e_1 = -1.065, e_2 = 0.0074, e_3 = -2×10^{-5}, e_4 = 1.32×10^{-5}	0.9971	0.9969	0.0081
	5.6	e_1 = -1.065, e_2 = 0.0083, e_3 = -3×10^{-5}, e_4 = 3.81×10^{-5}	0.9951	0.9948	0.147
	6.6	e_1 = -1.077, e_2 = 0.0097, e_3 = -3×10^{-5}, e_4 = 2.57×10^{-5}	0.9957	0.9954	0.0105

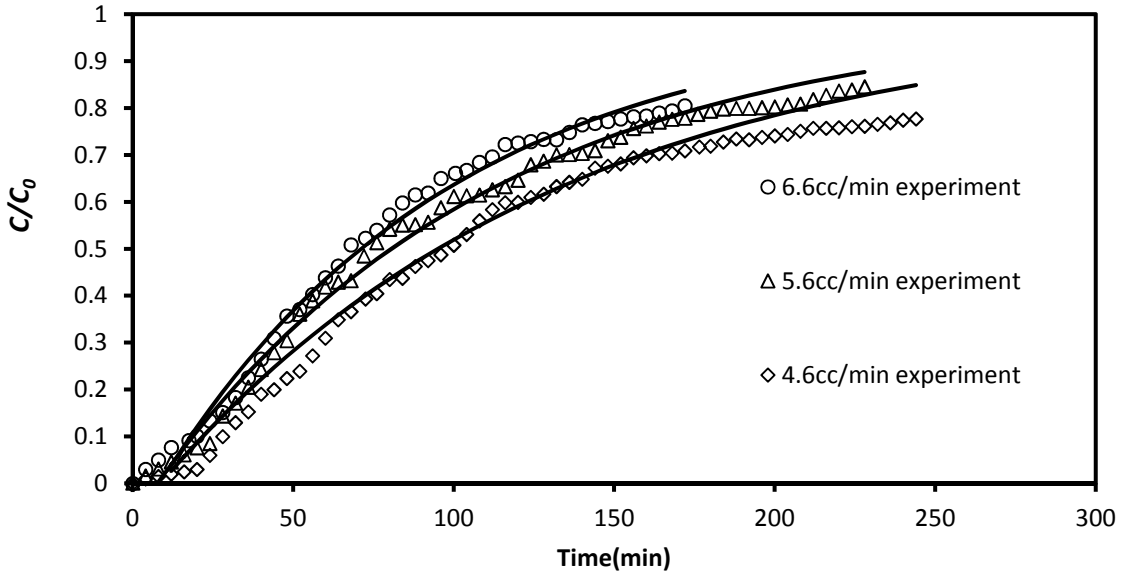

Figure 8: Experimental and predicted breakthrough curves of Model (1) (—— Predicted Model 1)

© 2013 Research Institute of Petroleum Industry (RIPI)

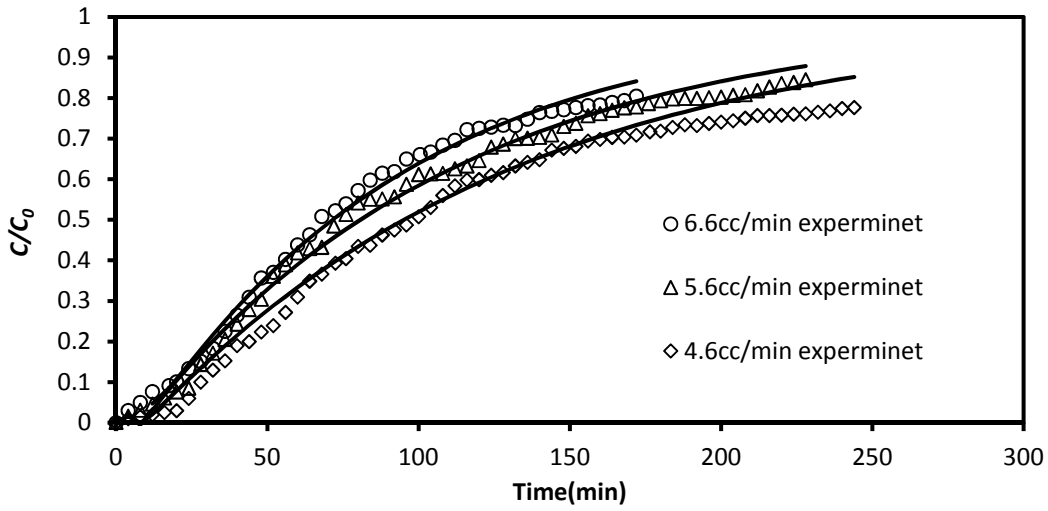

Figure 9: Experimental and predicted breakthrough curves of Model (2) (—— Predicted Model 2)

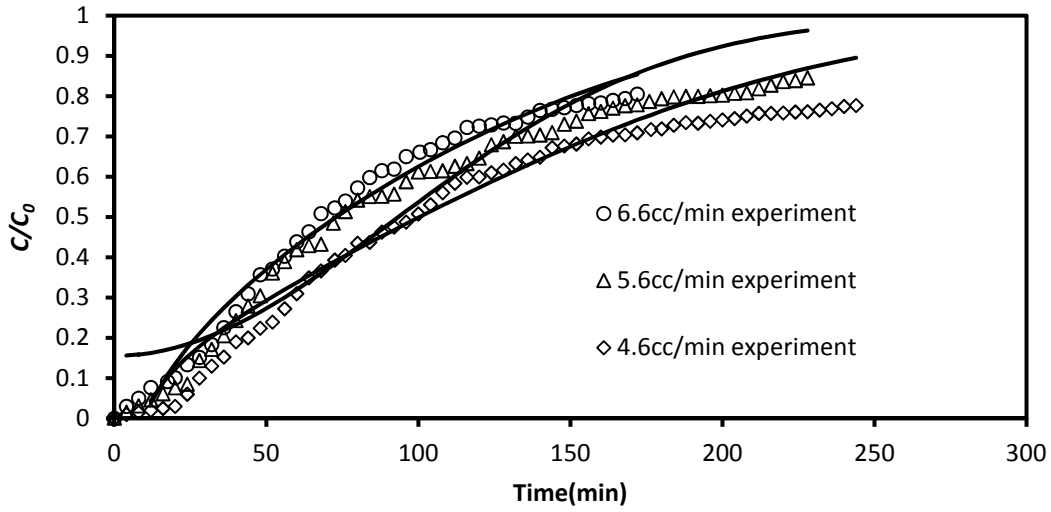

Figure 10: Experimental and predicted breakthrough curves of Model (3)) (—— Predicted Model 3)

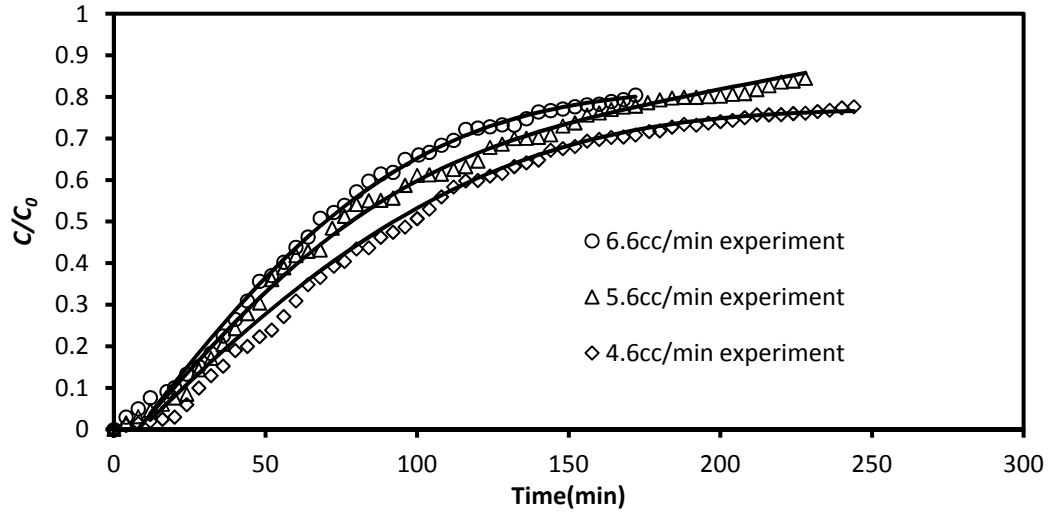

Figure 11: Experimental and predicted breakthrough curves of Model (4))(—— Predicted Model 4)

© 2013 Research Institute of Petroleum Industry (RIPI)

CONCLUSIONS

On the basis of the experimental results, TW was a great and novel sorbent for the removal of CR from aqueous solutions in a fixed-bed adsorption column. The adsorption process was found to perform better at a lower flow rate. The adsorption capacity increased from 1.53 to 1.78 mg/g by decreasing the flow rate from 6.6 to 4.6 mg/g. It was found that the presence of Fe_2O_3 nanoparticles significantly influenced the adsorption process, and thus the adsorption capacity increased by about 32% from 1.53 to 2.03 mg/g. The fixed-bed experimental data were analyzed using four different models. The results indicated that the models could properly predict the adsorption breakthrough curves.

REFERENCES

[1] Metivier-Pignon, H., Faur-Brasquet, C., Cloirec, P.L., "Adsorption of Dyes onto Activated Carbon Cloths: Approach of Adsorption Mechanisms and Coupling of ACC with Ultra Filtration to Treat Colored Wastewaters," *Sep. Purif. Technol*., **2003**, *31*, 3-11.

[2] O'Neill, C., Hawkes, F. R., Hawkes, D. L., Lourenco, N.D., Pinheiro, H. M., Delee, W. "Color in Textile Effluents – Sources, Measurement, Discharge Consents and Simulation: A Review," *J. Chem. Technol. Biotechnol*., **1999**, *74*, 1009-1018.

[3] Srinivasan, A., Viraraghavan, T., "Decolorization of Dye Wastewaters by Biosorbents: A Review," *J. Environ. Manage*., **2010**, *91*, 1915-1929.

[4] Song, J., Zou, W., Bian, Y., Su, F., Han, R. "Adsorption Characteristics of Methylene Blue by Peanut Husk in Batch and Column Models," *Desalination*., **2011**, *265*, 119-125.

[5] Gupta, V. K. Mittal, A. Krishnan, L. Gajbe, V. "Adsorption Kinetics and Column Operations for the Removal and Recovery of Malachite Green from Wastewater Using Bottom Ash," *Sep. Purif. Technol*., **2004**, *40*, 87-96.

[6] Jain, A. K. Gupta, V. K. Bhatnagar, A., "Utilization of Industrial Waste Products as Adsorbents for the Removal of Dyes," *J. Hazard. Mater*., **2003**, *101*, 31-42.

[7] Kulkarni, P. B. Bal, A. S. Bhole, A. G. Bhoi, A. V. "Color Removal by Granular Activated Carbon," *J. AWWA*., **1986**, *18*, 244-273.

[8] Gong, R. M. Ding, Y. Li, M. Yang, C. Liu, H. J. Sun, Y. Z. "Utilization of Powdered Peanut hull as Biosorbent for Removal of Anionic Dyes from Aqueous Solution," *Dyes Pigments*, **2005**, *64*, 187-192.

[9] Meyer, V. Carlsson, F. H. H. Oellermann, R. A. "Decolourization of Textile Effluent Using a Low Cost Natural Adsorbent Material," *Water Sci. Technol*., **1992**, *26*, 1205-1211.

[10] McKay, G. Ram Prasad, G. Mowli, P. "Desorption and Regeneration of Dye Colors from Low-cost Materials," *Water Res*., **1987**, *21*, 375-377.

[11] Perju, M. M. Dragan, E. S. "Removal of Azo Dyes from Aqueous Solutions Using Chitosan-based Composite Hydrogels," *Ion Exchange Lett*., **2010**, *3*, 7-11.

[12] Hameed, B. H., El-Khaiary, M. I., "Sorption Kinetics and Isotherm Studies of a Cationic Dye Using Agricultural Waste: Broad Bean Peels," *J. Hazard. Mater*., **2008**, *154*, 639-648.

[13] Calero, M., Hernainz, F., Blazquez, G., Tenorio, G., Martin-Lara, M. A.,"Study of Cr(III) Biosorption in a Fixed-bed Column," *J. Hazard. Mater*., **2009**, *171*, 886-893.

[14] Amarasinghe, B. M. W. P. K., Williams, R. A., "Tea Waste as a Low Adsorbent for the Removal of Cu and Pb from Wastewater," *Chem. Eng. J*., **2007**, *132*, 299-309.

[15] Wasewar, K. L., Atif, M., Prasad, B., Mishra, I. M., "Batch Adsorption of Zinc on Tea Factory Waste," *Desalination,* **2009**, *244*, 66-71.

[16] Malkoc, E., Nuhoglu, Y., "Investigations of Nickel(II) Removal from Aqueous Solutions Using Tea Factory Waste," *J. Hazard. Mater.,* **2005**, *127*, 120-128.

[17] Hameed, B. H., "Spent Tea Leaves: A New Non-conventional and Low-cost Adsorbent for Removal of Basic Dye from Aqueous

© 2013 Research Institute of Petroleum Industry (RIPI)

Solutions," *J. Hazard. Mater*., **2009**, *161*, 753-759.

[18] Lee, J. K., Koo, J., Hong, H., Kang, Y. T., "The Effects of Nanoparticles on Absorption Heat and Mass Transfer Performance in NH_3/H_2O Binary Nanofluids," *Int. J. Refrig*., **2010**, *33*, 269-275.

[19] Heyhat, M. M., Kowsary, F. Rashidi, A. M. Momenpour, M. H., Amrollahi, A., "Experimental Investigation of Laminar Convective Heat Transfer and Pressure Drop of Water-based Al_2O_3 Nanofluids in Fully Developed Flow Regime," *Exp. Therm Fluid Sci*., **2013**, *44*, 483-489.

[20] Masuda, H., Ebata, A., Teramae, K. Hishinuma, N., "Alterlation of Thermal Conductivity and Viscosity of Liquid by Dispersing Ultra-fine Particles (Dispersion of γ-Al_2O_3, SiO_2, and TiO_2 Ultra-fine Particles)," *Netsu Bussei*, **1993**, *7*, 227-233.

[21] Lee, S., Choi, S. U. S., Li, S., Eastman, J. A., "Measuring Thermal Conductivity of Fluids Containing Oxide Nanoparticles," *J. Heat Transfer*, **1999**, *121*, 280-289.

[22] Krishnamurthy, S., Bhattacharya, P., Phelan, P. E., Prasher, R. S., "Enhanced Mass Transport in Nanofluids," *Nano Lett*., **2006,** *6*, 419-423.

[23] Wen, J., Xiao, Q. J., Feng, W., "Hydrodynamic and Mass Transfer of Gas–liquid–solid Three-phase Internal Loop Airlift Reactors with Nanometer Solid Particles," *Chemical Engineering Technology*., **2005,** *28*, 53-60.

[24] Aksu, Z., Gönen, F., "Biosorption of Phenol By Immobilized Activated Sludge In A Continuous Packed Bed: Prediction Of Breakthrough Curves", *Process Biochem*. **2004**. 39, 599-613.

[25] Chen, S., Yue, Q., Gao, B., Li, Q., Xu, X., Fu, K., "Adsorption of Hexavalent Chromium from Aqueous Solution by Modified Corn Stalk: A Fixed-bed Column Study," *Bioresource Technol*., **2012**, *113*, 114-120.

[26] Albadarin, A. B., Mangwandi, C., Al-Muhtaseb, A. H., Walker, G. W., Allen, S. J., Ahmad, M. N. M., "Modelling and Fixed Bed Column Adsorption of Cr(VI) onto Orthophosphoric Acid-activated Lignin," *Chinese J. Chem. Eng*., **2012**, *20*, 469-477.

[27] Ahmad, A. A., Hameed, B. H. "Fixed-bed Adsorption of Reactive Azo Dye onto Granular Activated Carbon Prepared from Waste," *J. Hazard. Mater*., **2010**, *175*, 298-303.

[28] Malkoc, E., Nuhoglu, Y., "Removal of Ni(II) Ions from Aqueous Solutions Using Waste of Tea Factory: Adsorption on a Fixed-bed Column," *J. Hazard. Mater*., **2006**, *135*, 328-336.

[29] Malkoc, E., Nuhoglu, Y., "Potential of Tea Factory Waste for Chromium (VI) Removal from Aqueous Solutions: Thermodynamic and Kinetic Studies," *Sep. Purif. Technol.,* **2007**, *54*, 291-298.

[30] Vijayaraghavan, K., Jegan, J., Palanivelu, K., Velan, M., "Removal of Nickel(II) Ions from Aqueous Solution Using Crab Shell Particles in a Packed be up-flow Column," *J. Hazard. Mater*., **2004**, *113*, 223-230.

[31] Bohart, G. S., Adams, E. Q., "Behavior of Charcoal Towards Chlorine," *J. Chem. Soc*. **1920,** *42*, 523-529.

[32] Thomas, H. C., "Heterogeneous ion Exchange in a Flowing System," *J. Am. Chem. Soc*., **1944,** *66*, 1664-1466.

[33] Yoon, Y. H., Nelson, J. H., "Application of Gas Adsorption Kinetics: Part 1, A Theoretical Model for Respirator Cartridge Service Time," *Am. Ind. Hyg. Assoc. J*., **1984**, *45*, 509-516.

[34] Hutchins, R. A., "New Method Simplifies Design of Activated Carbon Systems," *Chem. Eng*., **1973**, *80*, 133-138.

[35] Kananpanah S., "Modeling of Mass Transfer at Adsorption Column by Using of Ion-exchange Resins," M. A. Thesis, University of Tehran, Iran, **2009**.

© 2013 Research Institute of Petroleum Industry (RIPI)